J Neurophysiol 106: 386–397, 2011.
First published May 4, 2011; doi:10.1152/jn.00018.2011.

Changes in the neural control of a complex motor sequence during learning

Bence P. Ölveczky,[1,2] Timothy M. Otchy,[2] Jesse H. Goldberg,[1] Dmitriy Aronov,[1] and Michale S. Fee[1]
[1]*McGovern Institute for Brain Research, Department of Brain and Cognitive Sciences, Massachusetts Institute of Technology, Cambridge; and* [2]*Department of Organismic and Evolutionary Biology and Center for Brain Science, Harvard University, Cambridge, Massachusetts*

Submitted 10 January 2011; accepted in final form 28 April 2011

Ölveczky BP, Otchy TM, Goldberg JH, Aronov D, Fee MS. Changes in the neural control of a complex motor sequence during learning. *J Neurophysiol* 106: 386–397, 2011. First published May 4, 2011; doi:10.1152/jn.00018.2011.—The acquisition of complex motor sequences often proceeds through trial-and-error learning, requiring the deliberate exploration of motor actions and the concomitant evaluation of the resulting performance. Songbirds learn their song in this manner, producing highly variable vocalizations as juveniles. As the song improves, vocal variability is gradually reduced until it is all but eliminated in adult birds. In the present study we examine how the motor program underlying such a complex motor behavior evolves during learning by recording from the robust nucleus of the arcopallium (RA), a motor cortex analog brain region. In young birds, neurons in RA exhibited highly variable firing patterns that throughout development became more precise, sparse, and bursty. We further explored how the developing motor program in RA is shaped by its two main inputs: LMAN, the output nucleus of a basal ganglia-forebrain circuit, and HVC, a premotor nucleus. Pharmacological inactivation of LMAN during singing made the song-aligned firing patterns of RA neurons adultlike in their stereotypy without dramatically affecting the spike statistics or the overall firing patterns. Removing the input from HVC, on the other hand, resulted in a complete loss of stereotypy of both the song and the underlying motor program. Thus our results show that a basal ganglia-forebrain circuit drives motor exploration required for trial-and-error learning by adding variability to the developing motor program. As learning proceeds and the motor circuits mature, the relative contribution of LMAN is reduced, allowing the premotor input from HVC to drive an increasingly stereotyped song.

motor control; zebra finch; songbird; vocal

MUCH OF OUR BEHAVIORAL REPERTOIRE is made up of learned motor sequences, yet little is known about how the control circuits underlying the acquisition of complex motor behaviors change during learning. The zebra finch, a songbird, provides an excellent model system for addressing this question. Like human infants learning to speak, juvenile birds start the process of song learning by uttering highly variable and unstructured vocalizations called subsong. Subsequently, in the plastic song stage, recognizable syllables emerge and develop, becoming less variable until the song crystallizes into adult song, a stereotyped sequence of reproducible syllables that resembles the tutor song the birds were exposed to early in life (see Figs. 1*B* and 3*A*) (Immelmann 1969; Tchernichovski et al. 1999).

According to the framework of trial-and-error learning (Sutton and Barto 1998), the variability of juvenile song may represent the motor exploration ("trial"), whereas the auditory feedback required for song learning (Konishi 1965) may allow the practicing bird to evaluate its vocal performance ("error") to guide learning (Doya and Sejnowski 1995; Tumer and Brainard 2007). To understand how song learning is implemented by the nervous system will require a description of how the neural signals that generate the song develop during learning.

Learned vocalizations are controlled by the descending "motor pathway" (Vu et al. 1994), a key nucleus of which is the robust nucleus of the arcopallium (RA), a motor cortex analog brain region that projects to brain stem nuclei controlling the vocal and respiratory muscles (Nottebohm et al. 1982; Vicario 1991; Wild 1997). During singing in adult birds, RA neurons generate highly stereotyped sequences of bursts that are tightly locked to the song (Leonardo and Fee 2005; Yu and Margoliash 1996). Two major inputs to RA come from premotor nucleus HVC (proper name) and the lateral magnocellular nucleus of the anterior nidopallium (LMAN), the output of an anterior forebrain pathway (AFP) that is homologous to mammalian basal ganglia-thalamocortical loops (Fig. 1*A*). LMAN is the cortex analog component of this forebrain loop. HVC neurons generate precisely timed bursts of activity that appear to directly drive the stereotyped sequence of bursts in RA during adult song (Hahnloser et al. 2002; Long and Fee 2008). Lesions to HVC have devastating effect on adult song (Nottebohm et al. 1976) but little effect on subsong (Aronov et al. 2008).

In contrast to HVC, LMAN plays a larger role in juvenile song than in adult song. LMAN lesions or pharmacological inactivations abolish subsong (Aronov et al. 2008) and largely eliminate song variability in plastic song (Ölveczky et al. 2005; Scharff and Nottebohm 1991) and adult song (Bottjer et al. 1984; Kao et al. 2005). The activity of LMAN neurons during singing is highly variable from rendition to rendition in both juvenile (Ölveczky et al. 2005) and adult birds (Hessler and Doupe 1999; Kao et al. 2008), leading to the suggestion that LMAN actively drives song variability through its excitatory projection to RA (Kao et al. 2005; Ölveczky et al. 2005; Stark and Perkel 1999).

To describe the development of the motor program underlying song, we recorded from RA neurons in singing juvenile zebra finches throughout the learning process, spanning from subsong to adult crystallized song. To examine how LMAN contributes to RA neuronal activity and vocal variability, we recorded from single RA neurons in singing juvenile birds while pharmacologically turning LMAN on and off during singing. Finally, we tested how HVC contributes to vocal stereotypy and RA neuronal activity by recording from RA neurons in adult birds with transections of the pathway from HVC to RA (Aronov et al. 2008). These manipulations allowed

Address for reprint requests and other correspondence: B. P. Ölveczky, Harvard Univ., 52 Oxford St., Rm. 219.30, Cambridge, MA 021398 (e-mail: olveczky@fas.harvard.edu).

us to dissect the relative contributions to the spiking activity in RA made by its two main inputs, HVC and LMAN, and to observe the neural correlates of vocal variability and stereotypy at the level of single neurons in RA.

METHODS

Subjects

Male zebra finches [$n = 13$ birds; 43–166 days posthatch (dph) during recording] were obtained from the MIT and Harvard zebra finch breeding facilities. The care and experimental manipulation of the animals were carried out in accordance with guidelines of the National Institutes of Health and were reviewed and approved by the MIT and Harvard Institutional Animal Care and Use Committees.

Surgery

Animals were anesthetized with 1.5–2% isoflurane in oxygen and placed in a stereotaxic apparatus (MyNeuroLabs). RA was localized stereotactically and further confirmed by electrophysiological criteria (Spiro et al. 1999). A custom-made lightweight (<1 g) motorized microdrive with three or four platinum-iridium electrodes (Microprobes; 5 or 10 MΩ) was implanted, targeting nucleus RA for recording (Fee and Leonardo 2001). In addition to the microdrive, custom-made microdialysis probes (<0.5 g) were implanted bilaterally into LMAN in three birds. To properly target the dialysis probes during surgery, LMAN was identified by antidromic activation from RA (Ölveczky et al. 2005). Both microdrive and dialysis probes were secured to the bird's skull using dental cement.

Reversible Inactivation of LMAN

Reversible inactivation was achieved by infusing lidocaine (2%), muscimol (0.1 mg/ml), GABA (100 mM), or tetrodotoxin (TTX; 5 μM) into microdialysis probes implanted into LMAN bilaterally. Unlike drug injections, microdialysis does not add volume to the brain; rather, it works by allowing diffusion of the inactivating agent into the targeted area. The probes through which the drug was infused had cylindrical dialysis membranes (210 μm in diameter, ~600 μm long) allowing for diffusion of the drug into LMAN (50-kDa cutoff). The probes for the two hemispheres were connected in series, and the drugs were infused with a syringe pump (WPI) connected to the probes through a fluid swivel (Instech) on the commutator used for the electrophysiological recordings (Crist Instruments) and FEP tubing (CMA Microdialysis). The joints between the inflow and outflow tubes and the probe were made using tubing adapters (CMA Microdialysis). The flow rate during drug infusion and washout was 2–4 ml/h. At other times saline was infused through the probes at 0.1 ml/h to prevent clogging of the outlet. Placement of the probes in LMAN was confirmed by histology. We assessed the effect of probe penetration on LMAN function by comparing song variability before and after implantation of a microdialysis probe in two juvenile birds (both 63 dph on the day of surgery) that resumed singing the day after surgery. This comparison showed no reduction in vocal variability (V) as a consequence of probe implantation in either bird [*bird 1*: $V = 0.40 \pm 0.11$ before vs. $V = 0.39 \pm 0.14$ after implantation; $n = 3$ syllables (mean ± SD); *bird 2*: $V = 0.39 \pm 0.12$ before vs. $V = 0.39 \pm 0.07$ after implantation; $n = 4$ syllables]. Nevertheless, we cannot rule out the possibility that the probes in LMAN affect its function, but based on our analysis this effect is likely small. The inactivation experiments were done in conjunction with microdrive recordings. Although we were careful to minimize the weight of the implanted devices, with our current approach it was not feasible to carry out these experiments in animals younger than 60 dph. Although the earliest successful implant occurred at 52 dph (the other birds used for this experiment were implanted at 57 and 65 dph, respectively), it usually took another week for birds to recover normal song output.

Chronic Neural Recordings in RA

Recordings were carried out using a motorized microdrive described previously (Fee and Leonardo 2001). Cells were isolated by searching for spontaneous spiking activity, and putative projection neurons were identified by their highly periodic firing patterns and large spike widths (Leonardo and Fee 2005; Spiro et al. 1999). We identified putative interneurons based on their low nonperiodic spontaneous spiking activity and their narrow spike widths (Leonardo and Fee 2005; Spiro et al. 1999). On the basis of these criteria, we recorded primarily projection neurons (146/150 neurons); only 4 of 150 neurons (~3%) were classified as putative interneurons. These were excluded from most of our analysis, and unless otherwise noted, reported quantities reflect only data from putative RA projection neurons. Neural and acoustic data were collected by custom-designed software written in MATLAB and LabView. For the cells in our data set, we recorded signals for many song motifs (range: 11–483 motifs). Single-unit recordings were made in the same bird for days to weeks (range: 1–48 days). The majority of recordings were made from birds that had identifiable sequences of syllables, allowing the alignment of the RA firing patterns to repeated syllable sequences (see Fig. 2). In addition, we carried out recordings from three subsong birds and two adult birds with HVC-RA fiber tract transections, none of which had identifiable syllables. Unless otherwise noted, all data refer to recordings made during undirected singing, i.e., songs produced during social isolation (Jarvis et al. 1998).

Transection of HVC Input to RA

Bilateral transections of the HVC-to-RA fiber tract were made by incisions with an ophthalmic knife (Sharpoint) at three locations in each hemisphere (~500 μm posterior to HVC, between 1.5 and 3.5 mm lateral, 2.5 mm maximum depth). The effectiveness of this procedure in severing connectivity between HVC and RA was previously documented using retrograde tracers (Aronov et al. 2008).

Data Analysis

Song analysis. Quantification of acoustic variability across renditions was done as by Ölveczky et al. (2005), using the Sound Analysis Pro Software package (Tchernichovski et al. 2000). Briefly, pairwise comparisons of the similarity of acoustic features of identified syllables were made. This score (S, ranging from 0 to 100) was converted, through a linear remapping, to a variability score (V) by the following formula:

$$V = \frac{S_{\max} - \langle S \rangle}{S_{\max} - \langle S_{\min} \rangle}$$

The quantity $\langle S_{\min} \rangle$ is the average similarity score of randomly chosen pairs of syllables from unrelated birds, which in our finch colony was measured to be 50 ± 12 (mean ± SD; $n = 200$ pairwise comparisons; comparisons were made across syllables of birds from different fathers). The similarity of identical syllables, $S_{\max}$, is 100 by definition of the similarity measure. Thus a variability score of 1 means that syllables are as different as two unrelated syllables, whereas a variability score of 0 means that the syllables are identical. Error bars for V all denote SE. $\langle V \rangle$ denotes the average variability score across birds and syllables for a given condition. Subsong is defined as song for which no syllables can be reliably identified from rendition to rendition.

Song alignment. In seven birds, neurons were recorded at a sufficiently advanced stage of plastic song that repeatable sequences of song syllables (motifs) could be identified (50–87 dph). This permit-

ted the calculation of spike train statistics that require alignment of spike trains across song renditions, such as trial-to-trial variability and sparseness. The sequence of song syllables most frequently produced by each bird was determined, and motifs that matched this sequence were identified and time-aligned using the onset of one of the syllables, usually the second syllable in the sequence. Our song alignment algorithm initially segregated syllables automatically using a threshold crossing of the acoustic power. Each syllable was then manually labeled based on similarity of the spectral derivative to a representative template syllable. If ambiguity arose as to the identity of a syllable, the entire motif was discarded.

In four birds, neurons were recorded during subsong or a sufficiently early stage of plastic song that syllables or sequences of syllables could not be identified (43–49 dph for 3 birds, 53 dph for a 4th bird). In these neurons, trial-to-trial variability and sparseness were not calculated.

Spike analysis. Spikes were sorted off-line using custom MATLAB software. All units included in the analysis had signal-to-noise ratios greater than 10:1. Single-unit signals were verified by a spike refractory period. Spikes were aligned to the chosen song motif. To account for the small trial-to-trial variability in song tempo, we used each syllable onset in the motif as an alignment point for the spike trains. Spike times between each alignment point were linearly stretched or compressed to match the corresponding intervals in a representative template motif (Leonardo and Fee 2005). To compensate for inaccurate motif alignment, we introduced a small temporal shift (from 0 to 15 ms in magnitude) in the spike trains to maximize the correlation between the smoothed spike trains (convolved with 8-ms Gaussian function) and the average motif-aligned firing pattern of the cell.

Spike train correlation. The precision of the song-aligned spike trains was measured using average pairwise correlation across all pairs of spike train for a given condition. Spike trains were converted into instantaneous firing rates $R(t)$ as follows:

$$R(t) = \frac{1}{t_{i+1} - t_i}; \quad \text{for} \quad t_i < t \leq t_{i+1},$$

where t_i is the ith spike. These instantaneous firing rates were then convolved with a 8-ms Gaussian function (Leonardo and Fee 2005), yielding a smoothed firing rate function $r(t)$. The correlation coefficient (CC) was then calculated between these firing rate functions for all pairs of spike trains as follows:

$$\mathrm{CC} = \frac{1}{N_{\text{pairs}}} \sum_{i}^{N} \sum_{j>i}^{N} \mathrm{CC}_{ij},$$

$$\mathrm{CC}_{ij} = \frac{\langle \hat{r}_i(t) \cdot \hat{r}_j(t) \rangle_t}{\sqrt{\langle \hat{r}_i(t)^2 \rangle_t \langle \hat{r}_j(t)^2 \rangle_t}},$$

where $\hat{r}(t)$ is the mean-subtracted smoothed firing rate function.

Burstiness

To quantify burstiness, we looked at the fraction of spikes contained within bursts (instantaneous rate >150 Hz). To explore the effect of LMAN on high-frequency bursts in RA, we considered spikes for which the instantaneous firing rate was above 400 Hz.

Sparseness

To quantify sparseness of a firing pattern, we used the entropy method (Lehky et al. 2005; Tolhurst et al. 2009), which gives a measure of how selective neural activity is for specific times in the song. For each neuron we calculated the song-aligned rate histogram (3-ms bins). Histograms were normalized to generate a time-varying probability spike-density function, p_i, where the ith value indicates the normalized firing probability for that time bin, such that $\sum_1^N p_i = 1$. We then computed the sparseness index (SI) as follows (Lehky et al. 2005):

$$\mathrm{SI} = 1 + \frac{\sum_{i=1}^{N} p_i \cdot \log(p_i)}{\log(N)}.$$

This index is 1 (maximal sparseness) when the activity is restricted to a single time bin and 0 if the spikes are evenly distributed across the time bins.

Postbout Suppression

Postbout suppression for RA neurons was calculated as the median time to the first spike after a song bout. Because song-related bursts sometimes extended ~10–20 ms into the postbout period, spikes within the first 30 ms after song termination were excluded. Song bout offsets were defined by the presence of at least 1 s of silence with no song syllables or calls. For 4 of the 39 cells recorded during undirected singing in adult birds, we did not record for sufficiently long times after bout termination to calculate a median time to first spike. These cells, which have a median time to first spike of at least 600 ms, were not included in Fig. 6. Thus our postbout suppression analysis in adult birds represents a lower bound for what is to be expected.

Significance

To determine significance of the trends we observed, we calculated the correlation coefficient between the given measure (e.g., sparseness, firing rate, etc.) and age of the birds. The P value of the correlation is the probability of getting a correlation as large as the observed value by random chance, when the true correlation is zero. To assess the significance of LMAN inactivation and age on various spike train metrics, we used Student's t-test. Our threshold for significance in both cases was $P < 0.05$.

RESULTS

In adult birds, the motor program underlying crystallized song is made up of highly stereotyped sequences of bursts in RA that are precisely timed-locked to the song (Leonardo and Fee 2005; Yu and Margoliash 1996). To determine how RA neurons encode the more variable songs of juvenile birds and how the motor program develops throughout learning, we recorded from a total of 150 RA neurons from 11 birds throughout song development and into adulthood (44–160 dph). The recorded cells fell into two functional classes based on their spontaneous firing patterns and spike shapes, consistent with previous classification as putative projection neurons and interneurons (Leonardo and Fee 2005; Spiro et al. 1999). In this article, we report on the 146 putative projection neurons (subsong: $n = 44$ cells, 4 birds, age range: 43–53 dph; plastic song: $n = 63$ cells, 7 birds, age range: 50–87 dph; adult song: $n = 39$, 2 birds, age range: 91–160 dph). We also compared our data to previously published recordings of RA firing patterns in older adult birds (>200 dph) singing directed songs to females ($n = 23$ cells, 3 birds) (Leonardo and Fee 2005). We do not include these data in the discussion of developmental trends (see below), instead restricting our analysis to birds singing in the same social context (i.e., undirected song).

RA Neurons Exhibit Increasing Burstiness During Song Development

The firing patterns of RA projection neurons in young birds with variable song were dramatically different from what has

been observed in adult birds (Figs. 1*B* and 2) (Leonardo and Fee 2005; Yu and Margoliash 1996). In subsong birds, RA neurons discharged sporadically and exhibited only occasional bursts (>150 Hz instantaneous firing rate), whereas in adult birds, almost all spikes discharged as part of bursts that reached considerably higher peak rates (Fig. 1*B*). These differences in firing pattern were visible in the aggregation of short intervals in the interspike interval (ISI) distributions, reflecting increased burstiness (Fig. 3*B*). The fraction of spikes in bursts (>150 Hz) increased during development from 45 ± 14% (n = 44 cells) in subsong birds to 84 ± 11% in adult birds (>90 dph; n = 39 cells) singing undirected song (Fig. 3*C*). The trend toward increased burstiness throughout the song learning phase (40–90 dph) was highly significant (R = 0.74; $P < 10^{-12}$).

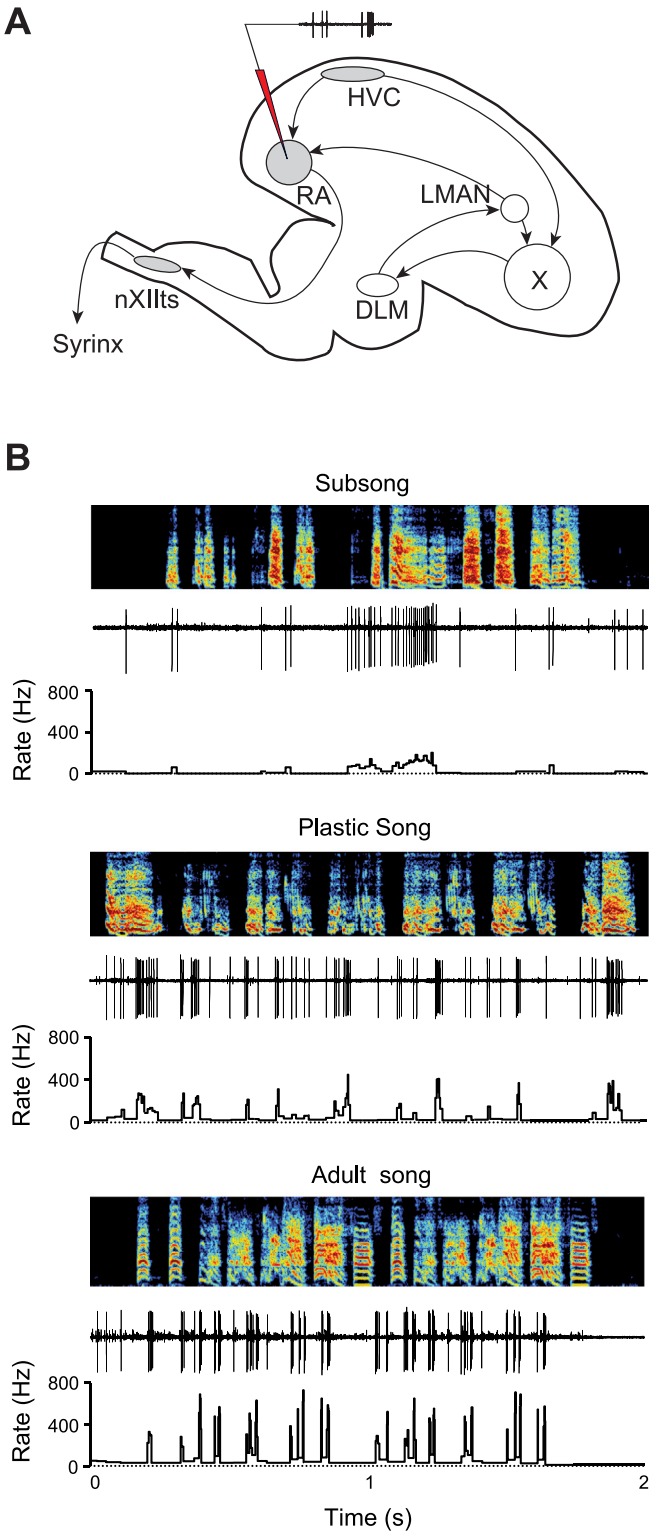

Fig. 1. Development of the robust nucleus of the arcopallium (RA) motor program in zebra finches. *A*: diagram showing the main pathways involved in song learning and song production. The motor pathway (gray) includes motor cortex analogs HVC and RA, whereas the anterior forebrain pathway (AFP; white), a basal ganglia thalamocortical circuit, consists of area X, the dorsolateral anterior thalamic nucleus (DLM), and the lateral magnocellular nucleus of the anterior nidopallium (LMAN), which, in turn, projects to RA. Chronic single-unit recordings in RA were carried out throughout sensorimotor learning and in adult birds. Syrinx, vocal organ; nXIIts, tracheosyringeal portion of the hypoglossal nucleus. *B*: development of song and the underlying RA firing patterns throughout song learning. Song spectrograms and corresponding raw traces of recorded RA neurons are shown at different developmental stages, subsong, plastic song, and adult song, in 3 different birds.

Emergence of Temporal Precision in RA Firing Patterns

As the song becomes more stereotyped with learning (Fig. 3*A*), the underlying motor program in RA similarly becomes more precise. We quantified temporal precision in plastic song birds, from the time the birds sang recognizable syllable sequences (motifs). Motif-aligned spike rasters were constructed to visualize how song-related spike patterns change during development (Fig. 2), and the correlation of neural activity with song timing was analyzed in two ways. First, to quantify how spiking was distributed across the motif, we computed a sparseness index SI, where a value of 1 indicates a neuron whose activity was entirely restricted to one part of the motif and a value of 0 indicates a neuron that spiked evenly across it (see METHODS). The SI increased during development from 0.083 ± 0.03 (n = 10) at 50–51 dph to 0.19 ± 0.05 in adult birds (90–160 dph; n = 39) singing undirected song (Fig. 3*E*), showing a significant correlation with age during song development (R = 0.69; $P < 10^{-10}$).

To quantify trial-to-trial variability in the firing rate modulations across multiple motif renditions, we computed pairwise cross correlations (CCs) between RA firing patterns during different motif renditions (see METHODS). CCs increased from 0.22 ± 0.1 (mean ± SD; n = 10 cells) at 50–51 dph to 0.81 ± 0.04 in adult birds (90–160 dph; n = 39) singing undirected song (Fig. 3*F*). The correlation between age and song-aligned spike train variability during song development was highly significant (R = 0.71; $P < 10^{-11}$; Fig. 3*F*).

The developmental trends observed at the population level were also observed in individuals. In one bird, recordings were made over several weeks (age range: 58–87 dph, n = 39 cells), and the trend toward more bursty, sparse, and precise RA firing patterns at later ages was highly significant (R = 0.57, P < 0.0003 for burstiness; R = 0.52, P < 0.001 for sparseness; R = 0.50, P < 0.002 for precision).

The average firing rate of RA neurons during singing also showed significant increase with age during learning (R = 0.52; $P < 10^{-11}$), almost doubling from 36.2 ± 22.8 Hz (mean ± SD; n = 44 cells) in subsong birds to 71.1 ± 25.0 Hz (n = 39) in adult bird singing undirected song. This suggests that the overall excitatory drive from RA projection neurons to down-

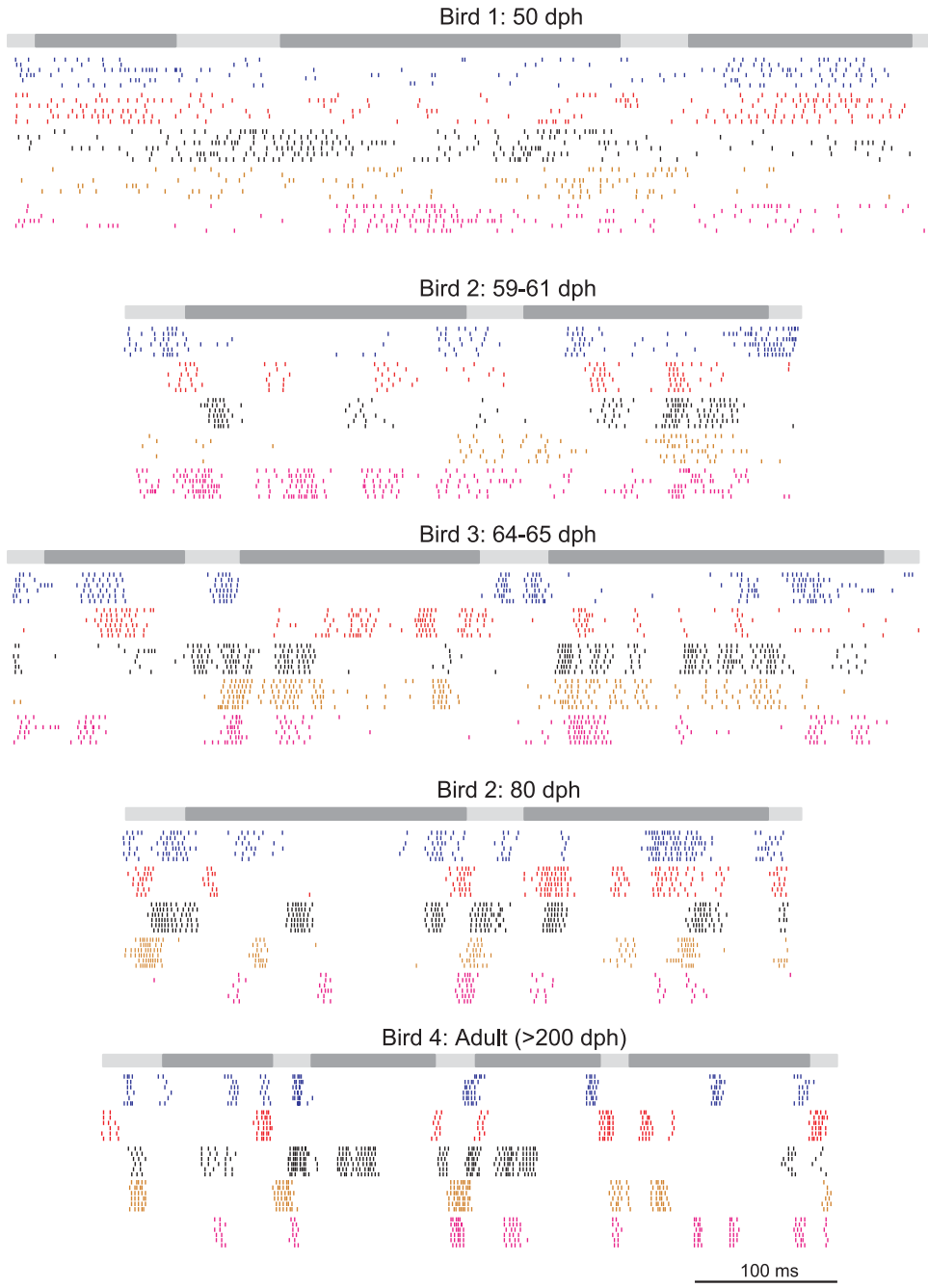

Fig. 2. Song-aligned firing patterns in RA neurons change gradually during learning. As the song becomes less variable and more similar to the tutor, the firing patterns in RA become more reproducible, sparse, and bursty. Raster plots show 5 representative RA projection neurons recorded at 5 different developmental time points. Each color represents a cell, and each row represents a rendition of the motif. Dark bars above the spike rasters indicate the beginning and end of identified syllables within each motif. For each developmental time point, the cells were recorded serially (i.e., not simultaneously). dph, Days posthatch.

stream target areas, as measured by average firing rates during singing, increases significantly throughout learning (Fig. 3*D*).

The trends seen in the maturation of the firing patterns reveal the functional reorganization of the motor circuits that accompanies song learning. To identify when the most significant changes occur, we compared our statistical measures for four age groups qualitatively ranging from subsong, through plastic song, to young adult song: *group I*, 43–49 dph ($n = 39$ from 3 birds); *group II*, 58–64 dph ($n = 19$ cells from 3 birds); *group III*, 79–87 dph ($n = 13$ cells from 2 birds); and *group IV*, 115–160 dph ($n = 17$ cells from 2 birds). The average statistics from neurons recorded in these age ranges are denoted by red squares in Fig. 3. There was a statistically significant increase in burstiness from *group I* to *group II* ($P < 10^{-7}$), from *group II* to *group III* ($P < 0.01$), and from *group III* to *group IV* ($P < 0.01$). Although the trend for the firing rate was very significant overall and doubled from subsong to early adult song, the incremental difference between adjacent developmental time points only reached significance when comparing *group II* with *group III* ($P < 0.005$).

For sparseness and precision measures, which are not quantified in subsong birds because they require alignment to song motifs, a slightly older age range was considered for *group I* (50–51 dph; $n = 10$ cells in 1 bird). Sparseness and precision increased significantly from *group I* to *group II* ($P < 10^{-4}$ and $P < 10^{-8}$, respectively) and also from *group II* to *group III* ($P < 0.02$ and $P < 0.05$, respectively). There was no statistically significant change for either of these metrics from *group III* to *group IV*. Together, our results show that although the most dramatic changes to the RA motor program occur in the

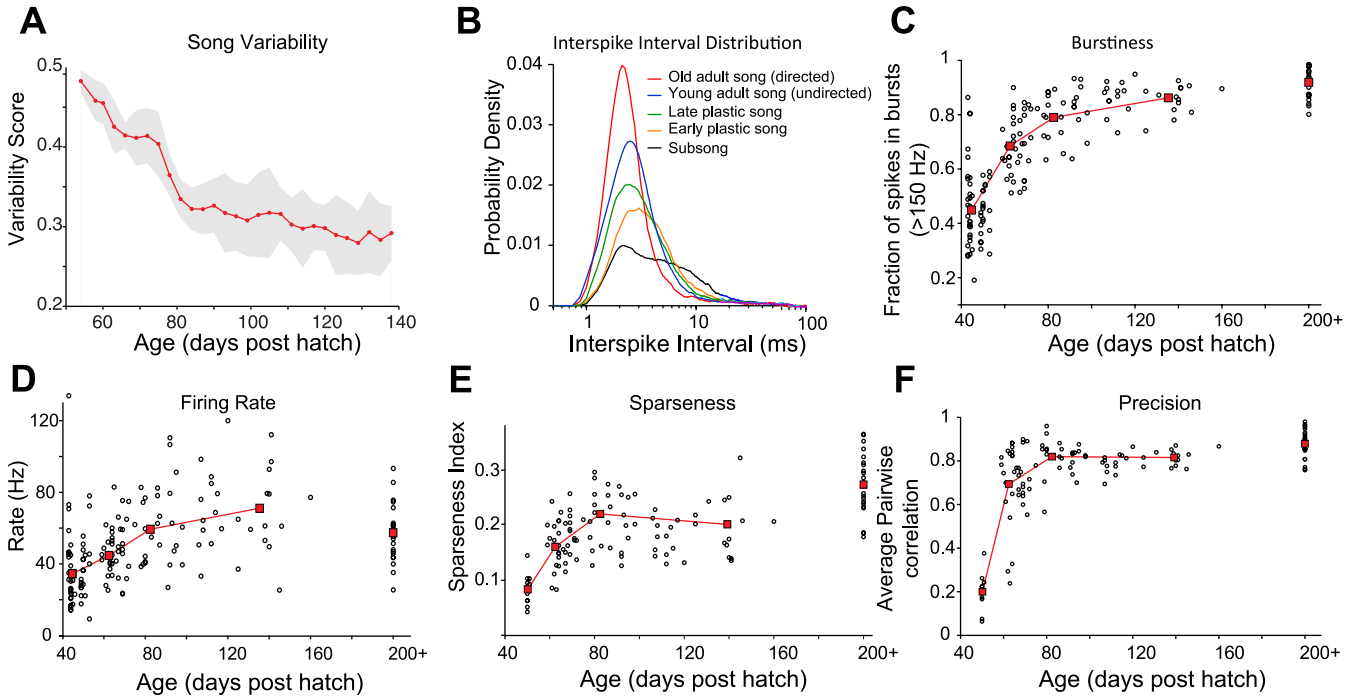

Fig. 3. Song learning, characterized by a decrease in song variability, is accompanied by changes in the statistics of RA projection neuron firing. *A*: acoustic variability as a function of age. Mean acoustic variability scores of readily identifiable syllables were calculated for 4 birds and averaged across birds. Shaded area denotes confidence interval ($P < 0.05$). *B*: interspike interval (ISI) distribution for birds at different ages throughout song development, corresponding roughly to subsong/early plastic song (43–49 dph), mid-plastic song (58–64 dph), late plastic song (79–87 dph), young adult song (115–160 dph), and older adult directed song (200+ dph). All ISI distributions were smoothed with an 8-ms square window. *C*: the fraction of spikes in bursts (>150 Hz). *D*: average firing rate during singing. *E*: sparseness index (see METHODS). *F*: average pairwise correlation of song-aligned spike trains. Black circles represent cells; red squares represent the average for different age groups described in *B*. (For *E* and *F*, the first point represents early plastic song at ages 50–51 dph; see METHODS).

first few weeks of sensorimotor learning (~40–60 dph), significant maturation of the RA firing patterns continues into adulthood. The neural correlate of song learning at the level of RA neurons can thus be described as a gradual change toward higher instantaneous firing rates in sparser and more precisely time-locked bursts.

Contribution of LMAN to RA Firing Patterns

We next explored the extent to which variability in RA neurons is driven from LMAN, the nucleus mediating the output of the AFP to RA. LMAN is involved in subsong production and in inducing song variability in plastic and adult song (Kao et al. 2005; Ölveczky et al. 2005), but it is not known how LMAN activity shapes the firing patterns in RA.

To test the hypothesis that LMAN drives variability in RA spiking and to explore how it does so, we recorded the activity of RA neurons during singing in juvenile birds first with LMAN intact and then with LMAN pharmacologically removed, leaving RA under the control of HVC, its other major input (Fig. 1*A*). We reasoned that comparing the firing patterns of RA neurons with and without LMAN during singing would reveal how inputs from HVC and LMAN contribute to variability in RA firing patterns and, in turn, the song itself.

To inactivate LMAN without disturbing the singing behavior or disrupting the neural recordings, we implanted microdialysis probes bilaterally into LMAN (Stepanek and Doupe 2010), allowing infusion of an inactivating agent. Because of its fast effects and quick reversal of action, most of our inactivations were done using lidocaine ($n = 14$ cells), but before settling on lidocaine as the optimal choice, we also used muscimol ($n = 1$ cell), GABA ($n = 1$ cell), and TTX ($n = 3$ cells). The effect on song variability using this method of inactivation was similar to that by bolus injections of TTX and muscimol into LMAN (Ölveczky et al. 2005), but reverse microdialysis afforded us significantly improved temporal control, achieving LMAN inactivation and a dramatic decrease in song variability in a matter of minutes without interfering with the bird's motivation to sing (Figs. 4, *A–C*). We recorded singing-related neural activity both with and without LMAN pharmacologically inactivated for at least 12 motifs in each condition (age range: 60–80 dph) for 19 RA neurons (18 putative projection neurons and 1 putative interneuron, see METHODS) in 3 birds.

Figure 4, *D–F*, shows three characteristic examples of how song-related RA firing patterns in juvenile birds were affected by LMAN inactivation. The overall activity patterns of putative RA projection neurons remained similar after LMAN inactivation as measured by the average correlation of the mean song-aligned firing patterns with and without drug infusion ($R = 0.92 \pm 0.06$), suggesting that during the age range of our recordings (60–80 dph), the RA motor program is predominantly driven from HVC. We found that the decrease in song variability produced by LMAN inactivation was always accompanied by a significant increase in the pairwise correlation of the song-aligned spike trains of RA projection neurons (0.71 ± 0.2 with LMAN active vs. 0.89 ± 0.08 with LMAN inactivated; $P < 10^{-4}$ for all cells; see Fig. 5, *A* and *B*, for an example and *C* for population data). This correlation was significantly higher in LMAN-inactivated plastic song birds than in adult birds (with intact LMAN) singing undirected song

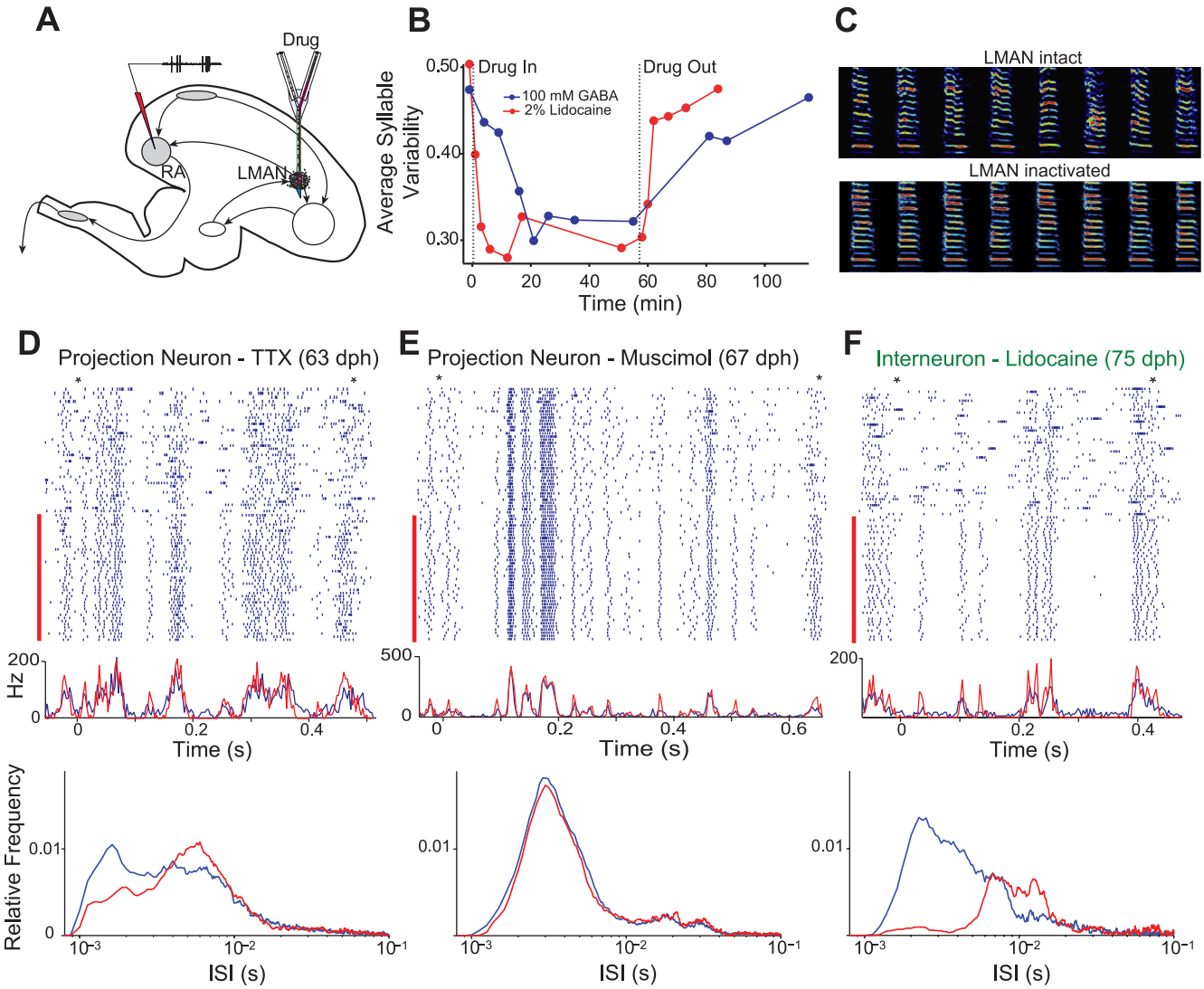

Fig. 4. Transient inactivation of LMAN decreases variability of RA activity patterns and vocal output. *A*: experimental setup. Recordings were made from RA neurons while LMAN was inactivated using reverse microdialysis (see METHODS). *B*: behavioral effect on acoustic variability following infusion of GABA and lidocaine into the dialysis probes implanted bilaterally in LMAN. Each data point was calculated from 10 renditions of 4 identified syllables (see METHODS) in a single bird (73 and 74 dph for GABA and lidocaine, respectively). *C*: 8 consecutive renditions of a syllable before (LMAN intact) and during 2% lidocaine infusion (LMAN inactivated). *D–F*, *top*: song-aligned raster plots of spike trains of 2 representative RA projection neurons (*D* and *E*) and 1 interneuron (*F*). Time advances from *top* to *bottom*; red bar indicates recordings during LMAN inactivation. To better contrast the 2 conditions, the period of drug wash-in (0–20 min after start of infusion) is not shown. Other than for the period of drug infusion, the shown spike trains were recorded during consecutive renditions of the song motif. Asterisks denote the start and end of the song motif to which the spike trains were aligned. Below the spike trains are the song-aligned histograms for the neurons. *D–F*, *bottom*: changes in the ISI distribution as a consequence of LMAN inactivation (red line, LMAN inactivated; blue line, LMAN intact). As is evident from the spike rasters above, LMAN can introduce high-frequency bursts into the RA firing patterns, and thus LMAN inactivation shifts the distribution toward longer ISIs. Reduction in high-frequency bursts (>400 Hz) for the 3 cells shown was 43, 21, and 90%, respectively. TTX, tetrodotoxin.

(0.82 ± 0.04; $n = 17$ cells from birds 115–160 dph; $P < 0.005$) but statistically similar to adult birds singing directed song (0.88 ± 0.07; $n = 23$ cells; $P > 0.8$). This is consistent with recent results showing that LMAN regulates social context-dependent changes in song variability (Stepanek and Doupe 2010).

Moreover, for 15 of 18 projection neurons, the song-aligned spike trains recorded with LMAN active were significantly ($P < 0.01$) less correlated with each other than they were with spike trains recorded with LMAN inactivated (Fig. 5*C*), implying that LMAN adds variability around a core motor program generated by the descending motor circuit. This effect was seen also at the behavioral level (Fig. 5*B*): the song with LMAN intact was more similar, on average, to the core song produced without LMAN active than to other renditions of the song with LMAN active. The stereotypy of the RA motor program after LMAN inactivation further suggests that HVC, the main premotor input to RA, provides a temporally precise input sequence to RA already early in song learning (Hahnloser et al. 2002).

Although LMAN inactivations always increased the stereotypy of RA firing patterns (Fig. 5*C*), there was a range of effects among the putative projection neurons, as measured by the difference in average pairwise correlation of the song-aligned spike trains before and during inactivation. This effect was strongly predicted ($R = -0.97$; $P < 10^{-12}$) from the spike train correlation before inactivation; i.e., the more variable the spike trains were initially, the larger the

effect of LMAN inactivation (Fig. 5*C*). There was also a significant anti-correlation of the effect of LMAN inactivation with burstiness ($R = -0.51$; $P < 0.03$), firing rate ($R = -0.48$; $P < 0.04$), and sparseness ($R = -0.48$; $P < 0.04$). Although the effect of LMAN inactivation showed a tendency to decrease with age, in our data set this trend did not reach significance ($R = -0.35$; $P = 0.13$). Determining more explicit age-related effects of LMAN inactivations requires recordings from younger birds, something that our current methodology did not allow (see METHODS). Thus the effect of LMAN inactivation on the song-aligned firing patterns of RA projection neurons, as measured by an increase in the average pairwise spike train correlation, depended significantly on the structure and statistics of the RA spike trains: neurons that were relatively less sparse, less bursty, and had lower firing rate were most strongly affected by the variable input from LMAN.

One way in which LMAN contributes to the variability was revealed by comparing the ISI distributions of RA projection neurons before and after LMAN inactivation. The small but significant increase in the occurrence of short ISIs with LMAN active (Fig. 4, *D–F*, *bottom*, and Fig. 5*E*) suggests that LMAN acts to introduce variability into the motor program by adding high-frequency bursts to the activity patterns of RA neurons. The relative fraction of spikes in high-frequency bursts (>400 Hz) showed an average decrease of 22 ± 32% after LMAN

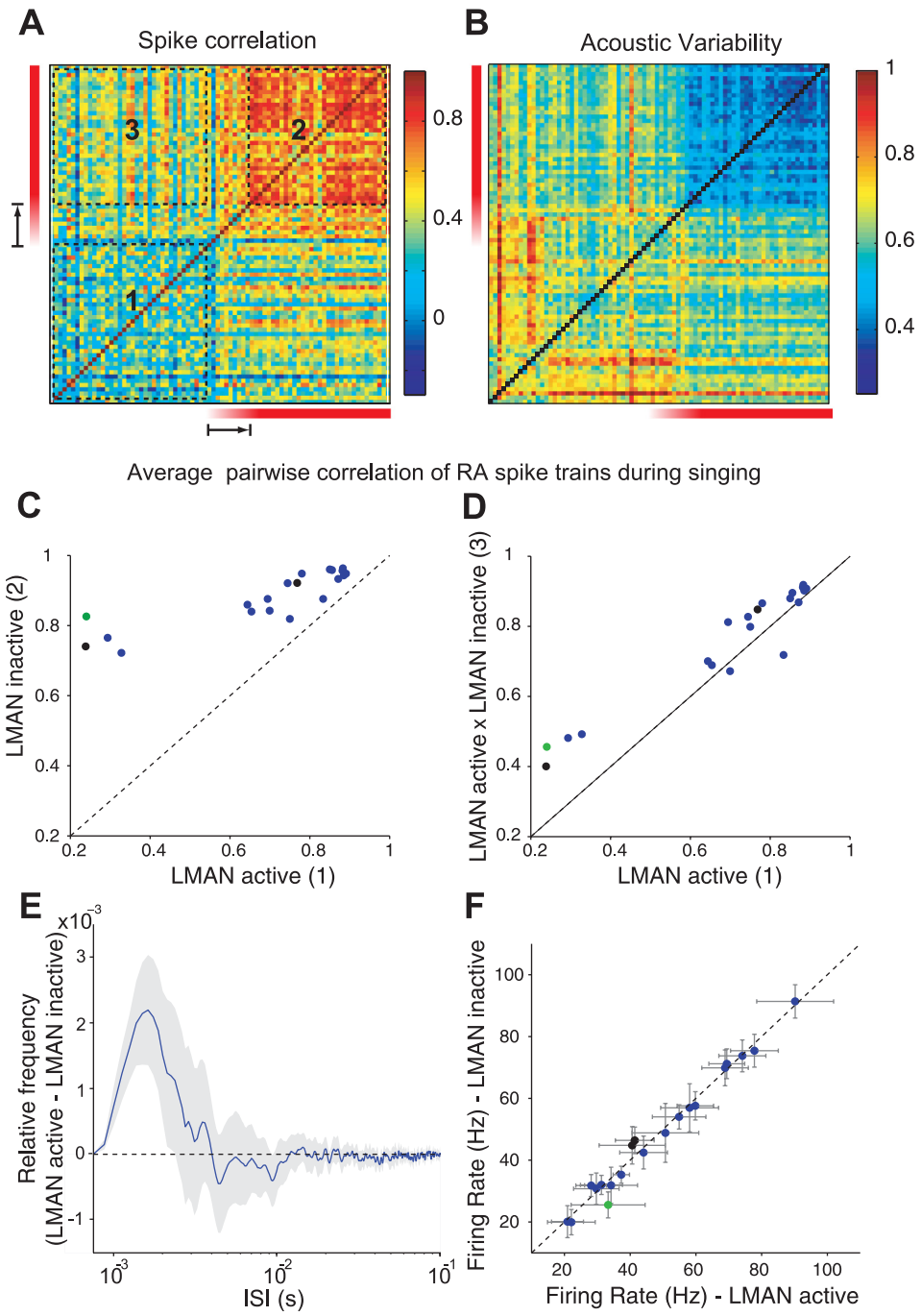

Fig. 5. Effects of LMAN inactivation on the RA motor program and song. *A*: matrix of pairwise spike train cross-correlations across different renditions for the neuron represented in Fig. 4*D*. Note the increased correlation after LMAN inactivation (red bar). *B*: matrix of pairwise song similarity scores across different renditions, corresponding to the motifs in *A*. The bird sang throughout the drug wash-in period (denoted by arrow), and the gradual shift toward more stereotypy can be seen in both the acoustic similarity and spike correlation. *C*: average spike train correlation for the RA cell population with and without LMAN active. Referencing the matrix in *A*, the graph depicts the average correlation in *quadrant 1* vs. *quadrant 2* for all neurons. *D*: pairwise correlation between spike trains in RA with LMAN intact and spike trains with LMAN silenced (*quadrant 3* in *A*) is higher than the correlation between spike trains with LMAN intact (*quadrant 1* in *A*). *E*: the difference in ISI distribution across the population of projection neurons ($n = 18$ cells) with and without LMAN active reveals a net increase in short ISIs with LMAN activity. Shaded area denotes confidence interval ($P < 0.05$). ISI distributions were smoothed with an 8-ms square window. *F*: average firing rate for projection neurons is similar with and without LMAN active. For *C*, *D*, and *F*, black data points denote the projection neurons in Fig 4, the whereas the green data point represents the interneuron. Error bars denote SD.

inactivation (range: −16–72%). There was a significant decrease in high-frequency bursts for 9 of the 18 projection neurons and a small but significant increase for 3 neurons. The contribution of LMAN input to RA was particularly visible in the firing pattern of one putative interneuron, for which the average pairwise spike train CC went from 0.24 to 0.83, and the fraction of spikes in high-frequency bursts (>400 Hz) decreased by 90% after LMAN was inactivated (Fig. 4*F*). The interneuron, which also differed from the projection neurons in other ways (Fig. 5), was not included in the population analysis.

Even though LMAN provides direct excitatory input to RA neurons (Mooney 1992), average firing rates of projection neurons were not consistently altered by silencing LMAN (Fig. 5*F*), showing, on average, a 0.2% ± 6.0% increase after LMAN inactivation (range: −11.6–10.9%). The firing rate was only significantly different ($P < 0.05$) for 6 of 18 cells, and even for those the trend was ambiguous, with 2 cells increasing and 4 decreasing their firing rates when LMAN was inactivated. Although speculative, this suggests that the loss of excitatory LMAN input to RA projection neurons is counterbalanced by a decrease in the recurrent or feedforward inhibition activated by LMAN inputs (Spiro et al. 1999), which could serve to keep the overall level of RA output constant irrespective of LMAN activity.

Contribution of HVC Input to RA Firing Patterns

Bilateral HVC lesions or surgical transection of the HVC-to-RA pathway has been shown to eliminate normal adult song (Aronov et al. 2008; Nottebohm et al. 1976). However, adult birds with these manipulations produce vocalizations that closely resemble normal subsong (Aronov et al. 2008). We reasoned that examining RA firing patterns in the absence of HVC input would offer further insight into the respective contributions made by HVC and LMAN to RA firing patterns. We recorded from RA neurons in adult birds that had the fiber pathway from HVC to RA surgically severed ($n = 10$ cells from 2 birds; see METHODS) and found the song-related RA firing patterns to be similar to those recorded in normal subsong birds (Fig. 6), in terms of both the overall ISI distribution and the average firing rate (36.2 ± 22.8 Hz for subsong birds vs. 34.1 ± 6.2 Hz for adult transected birds; $P > 0.75$). However, the burstiness of RA neurons in the transected birds was even lower than for those recorded during subsong (Aronov et al. 2008) (45 ± 14% of spikes were in bursts for subsong birds vs. 24 ± 6% for adult transected birds; $P < 10^{-4}$), reflecting either an age-related difference in the effectiveness with which LMAN activity drives bursting in RA neurons or a contribution of HVC inputs to RA even during subsong.

The transections revealed another surprising contribution of HVC to RA firing patterns. RA neurons exhibit characteristic tonic spiking during nonsinging that in adult birds is suppressed at the end of song bouts (Yu and Margoliash 1996). We found that, in some neurons, this suppression lasts for close to a second, and on average, the median time from the bout offset to the occurrence of the first spontaneous spike in young adult birds singing undirected song was 0.39 ± 0.19 s. Transection of the HVC-to-RA fiber tract in adult birds caused a dramatic shortening of the average time from bout offset to the occurrence of the first spike (median: 0.07 ± 0.04 s; $P < 10^{-5}$ compared with intact adult), reducing the duration of postbout suppression of spontaneous activity to levels similar to that seen in subsong birds (median: 0.15 ± 0.15 s; $P > 0.1$, transected vs. subsong).

DISCUSSION

This study was aimed at understanding how the motor program underlying a complex, learned motor sequence evolves through learning and how the behavioral variability underlying trial-and-error motor learning is represented and expressed in the brain. Our experiments focused on the motor representation in the primary motor cortex analog brain region RA of juvenile zebra finches and have revealed for the first time the evolution of a complex acquired motor program throughout learning at the single-neuron level. We have shown that the sparse and precise motor program that underlies the stereotyped vocal performance of adult birds emerges and matures throughout the sensorimotor phase of song learning (Fig. 2). As learning progresses, the precision, burstiness, and sparseness of RA firing increase (Fig. 3).

Our results, describing the maturation of the motor program in RA, raise questions about the neural circuit mechanisms underlying these developmental changes. Synaptic reorganization at the HVC-to-RA synapse is known to occur as a consequence of learning (Herrmann and Arnold 1991; Kittelberger and Mooney 1999) and likely causes learning-related changes in RA firing patterns. If indeed RA bursts are driven from HVC (Hahnloser et al. 2002), the reported increase in the strength of those synaptic inputs is likely to contribute to the trends we report. Previous studies (Crandall et al. 2007; Day et al. 2008) have examined multiunit activity in HVC in juvenile zebra finches. These studies suggest that the trends in the firing patterns observed in RA during learning may, at least to some degree, be caused by developmental changes in the premotor input from HVC. Whether the changes in the RA synaptic network and in HVC are driven by experience-dependent learning or whether they are under developmental control remains to be seen.

Another interesting finding was that the firing rate of RA neurons was largely unaffected by removing the excitatory input from LMAN, suggesting that the inhibitory and excitatory networks in RA are well balanced to ensure that a change in LMAN input does not dramatically affect the overall motor output. The LMAN-dependent inhibition may come from RA interneurons (the recording of 1 putative inhibitory interneuron showed a very significant 24% drop in firing rate after LMAN inactivation). Balancing excitation and inhibition may be important for song maintenance in adult birds: the structure of LMAN firing depends on social context, with LMAN spike trains being considerably more bursty when the song is directed to a female than when it is undirected (Kao et al. 2008). Given that most of LMAN input is through *N*-methyl-D-aspartate (NMDA)-type glutamate receptors (Stark and Perkel 1999), a burstier LMAN input is likely to provide more excitatory drive. Having a self-regulating mechanism that can counter the social context-induced changes in excitation with proportional changes in inhibitory input to RA projection neurons would ensure that the overall RA drive to the muscles is similar in the two conditions.

We further observed what appears to be a developmental increase in the inhibitory tone of RA neurons. Early in plastic

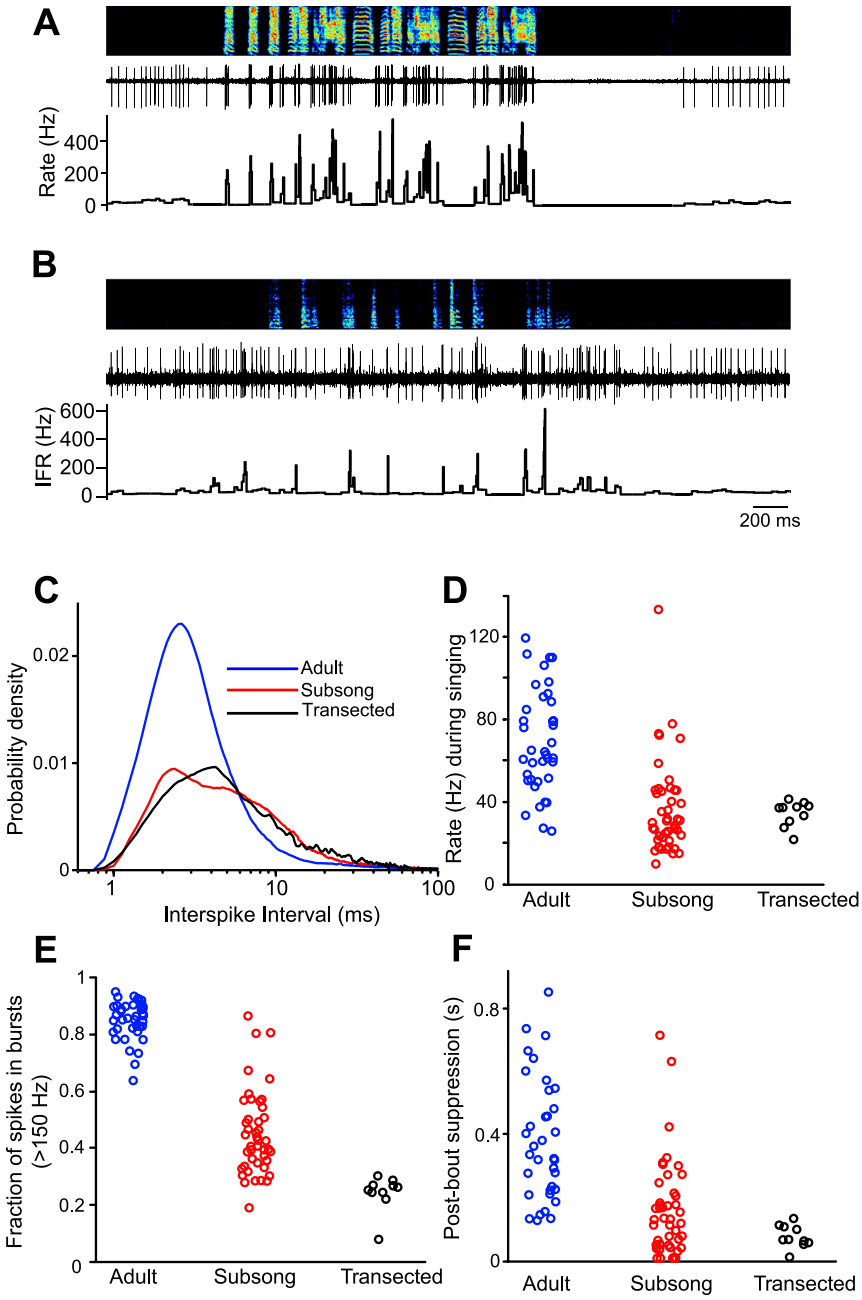

Fig. 6. Firing patterns in RA projection neurons revert to a subsonglike state following the elimination of inputs from HVC. *A*: recording of a single neuron in RA (black trace) during undirected singing in an adult bird. *B*: recording of an RA neuron during undirected singing in an adult bird following complete bilateral transection of the HVC-to-RA fiber tract. *C*: ISI distributions of neurons recorded in intact adult birds, subsong-producing birds, and adult birds following transection. *D*: mean firing rate of each neuron recorded in intact adult birds, subsong birds, and adult bird following transection. *E*: fraction of spikes contained in bursts (>150 Hz instantaneous firing rate). *F*: duration of spiking suppression after singing. Each data point is the median time of the first spike after bout offset.

song, RA neurons tended to be active throughout the song (Fig. 2), without consistent song-locked periods of spiking inhibition. As the song developed, RA firing patterns were increasingly characterized by high-frequency bursts separated by periods of silence. The low probability of interburst spiking in adult birds during singing suggests that RA neurons may be strongly hyperpolarized during these periods. This inhibition appears to continue even after the song stops, as evidenced by a suppression of tonic activity for several hundred milliseconds after bout offset in adult birds (Fig. 6) (Yu and Margoliash 1996).

The singing-related inhibitory tone of RA neurons could be produced by slow inhibitory conductances, possibly mediated by the inhibitory network in RA (Spiro et al. 1999), or even more directly by the action of glutamatergic inputs from HVC. For example, a similar postbout spiking suppression in HVC (Schmidt and Perkel 1998) has been attributed to activation of potassium currents by metabotropic glutamate receptors (Dutar et al. 2000). The dramatic reduction of postbout spike suppression we observed following transection of the HVC-to-RA fiber tract suggests that excitatory drive from HVC mediates the inhibitory tone of RA neurons. Thus increased excitatory inputs to RA from HVC during development (Kittelberger and Mooney 1999) could also gradually increase the inhibitory tone of RA neurons.

Removing the descending HVC input to RA in adult birds resulted in RA firing patterns and song output similar to that observed in subsong birds (Fig. 6), suggesting that the functional connections between LMAN and RA are not fundamentally altered during learning. Rather, it is the effectiveness by which LMAN drives variability in RA that changes. Such a decrease in LMAN's ability to influence the RA motor program could be

explained by the developmental increase in the inhibitory tone of RA neurons described above. Increased inhibition could selectively suppress the primarily NMDA-receptor-mediated LMAN synaptic inputs (Mooney and Konishi 1991) due to the voltage dependence of NMDA receptors (Nowak et al. 1984). In contrast, this inhibition would have little effect on the *dl*-α-amino-3-hydroxy-5-methylisoxazole propionic acid (AMPA)-receptor-mediated HVC inputs (Mooney and Konishi 1991; Stark and Perkel 1999). Consistent with this idea, infusion of an NMDA-type glutamate receptor blocker (APV) into RA in plastic song birds has little effect on average song structure but largely abolishes song variability (Ölveczky et al. 2005). The role of inhibition in modulating LMAN-driven inputs to RA can be tested experimentally by recording and manipulating the membrane potential of RA neurons intracellularly during singing (Long et al. 2010).

Developmentally increased excitatory drive from HVC to RA (Kittelberger and Mooney 1999) may also reduce the effectiveness of LMAN input when an RA neuron is active. In older birds the strong excitatory input from HVC drives high-frequency bursts in RA, leaving little room for additional firing rate modulation by LMAN. Thus the decreasing effectiveness of LMAN inputs during development could arise as a consequence of an increasing synaptic drive to RA from HVC, leaving RA neurons in older birds either too hyperpolarized or too saturated for LMAN inputs to have a significant effect. Consistent with this hypothesis, small lesions of HVC result in increased LMAN-dependent song variability (Thompson and Johnson 2007), possibly as a direct consequence of a loss of excitatory drive from HVC to RA.

The effectiveness of LMAN in driving song variability may also be under the control of neuromodulatory inputs to RA. Specifically, norepinephrine (NE) has been shown to diminish the efficacy of LMAN inputs to RA neurons in vitro (Perkel 1995) while increasing the signal-to-noise ratio of HVC inputs to RA (Solis and Perkel 2006), resulting in a reduced AFP influence on the motor pathway. This raises the possibility that the developmental reduction of LMAN-driven variability could be under neuromodulatory control. However, this idea is at odds with our results showing rapid restoration of LMAN's effectiveness in generating variability in both song and RA firing patterns following transection of the RA-projecting HVC fibers in adult birds and with the observation that NE levels decrease with age (Harding et al. 1998). The extent to which the above-mentioned circuit mechanisms (i.e., neuromodulation and inhibitory tone of RA neurons) contribute to the reduction in variability will require further examination.

We found that, in older juvenile birds, LMAN acts to introduce variability into the RA firing patterns without introducing large changes in the average song-related firing rate patterns of the projection neurons (Fig. 4). This observation may at first appear to contradict recent results showing that LMAN biases vocal output in the direction of reduced error (Andalman and Fee 2009). Indeed, under the conditions in which these recordings were carried out, LMAN appears to introduce variability in RA neurons around a core motor program driven by HVC. We point out, however, that the large AFP bias found in the aforementioned study (Andalman and Fee 2009) was observed during rapid learning induced by a conditional auditory feedback (CAF) learning paradigm. In that study, LMAN inactivation in the absence of CAF produced no significant change in the average acoustic structure of the song, suggesting that under normal learning conditions, AFP bias is small. That LMAN does not appear to drive large changes in the average firing patterns of RA neurons in our data set is consistent with a small AFP bias. A test of the idea that LMAN drives consistent changes in the RA firing patterns to bias vocal output would require measurements to be made during CAF or possibly during periods of rapid learning induced by tutor exposure (Tchernichovski et al. 2001).

Our findings add mechanistic detail to the conceptual model suggested by recent studies examining the role of LMAN and HVC in song learning (Aronov et al. 2008; Kao et al. 2005; Ölveczky et al. 2005). Early in learning, the AFP drives highly variable patterns of activity in RA through LMAN, resulting in unstructured and variable subsong (Aronov et al. 2008). As HVC starts innervating RA at around *day 35* posthatch (Mooney, 1992), this premotor input begins to drive stereotyped sequences of bursts in RA, to which LMAN input adds variability. As learning proceeds, the influence of LMAN on RA is diminished and the control shifts to HVC, resulting in a progressively more stereotyped song.

GRANTS

This work was supported by National Institutes of Health Grants R01 DC009183 (M. S. Fee) and R01 NS66408 (B. P. Ölveczky). Additional support was provided by the Damon Runyon Foundation and Charles King Trust Postdoctoral Fellowships (J. H. Goldberg), the Klingenstein and McKnight Foundations (B. P. Ölveczky), and the Hertz Foundation (D. Aronov).

DISCLOSURES

No conflicts of interest, financial or otherwise, are declared by the author(s).

REFERENCES

Andalman AS, Fee MS. A basal ganglia-forebrain circuit in the songbird biases motor output to avoid vocal errors. *Proc Natl Acad Sci USA* 106: 12518–12523, 2009.

Aronov D, Andalman AS, Fee MS. A specialized forebrain circuit for vocal babbling in the juvenile songbird. *Science* 320: 630–634, 2008.

Bottjer SW, Miesner EA, Arnold AP. Forebrain lesions disrupt development but not maintenance of song in passerine birds. *Science* 224: 901–903, 1984.

Crandall SR, Aoki N, Nick TA. Developmental modulation of the temporal relationship between brain, and behavior. *J Neurophysiol* 97: 806–816, 2007.

Day NF, Kinnischtzke AK, Adam M, Nick TA. Top-down regulation of plasticity in the birdsong system: "premotor" activity in the nucleus HVC predicts song variability better than it predicts song features. *J Neurophysiol* 100: 2956–2965, 2008.

Doya K, Sejnowski T. A novel reinforcement model of birdsong vocalization learning. In: *Advances in Neural Information Processing Systems 7*, edited by Tesauro G, Touretzky DS, Leen T. Cambridge, MA: MIT Press, 1995, p. xxi.

Dutar P, Petrozzino JJ, Vu HM, Schmidt MF, Perkel DJ. Slow synaptic inhibition mediated by metabotropic glutamate receptor activation of GIRK channels. *J Neurophysiol* 84: 2284–2290, 2000.

Fee MS, Leonardo A. Miniature motorized microdrive, and commutator system for chronic neural recording in small animals. *J Neurosci Methods* 112: 83–94, 2001.

Hahnloser RH, Kozhevnikov AA, Fee MS. An ultra-sparse code underlies the generation of neural sequences in a songbird. *Nature* 419: 65–70, 2002.

Harding CF, Barclay SR, Waterman SA. Changes in catecholamine levels, and turnover rates in hypothalamic, vocal control, and auditory nuclei in male zebra finches during development. *J Neurobiol* 34: 329–346, 1998.

Herrmann K, Arnold AP. The development of afferent projections to the robust archistriatal nucleus in male zebra finches: a quantitative electron microscopic study. *J Neurosci* 11: 2063–2074, 1991.

Hessler NA, Doupe AJ. Singing-related neural activity in a dorsal forebrain-basal ganglia circuit of adult zebra finches. *J Neurosci* 19: 10461–10481, 1999.

Immelmann K. Song development in the zebra finch, and other etrilid finches. In: *Bird Vocalizations*, edited by Hinde RA. New York: Cambridge University Press, 1969, p. 61–74.

Jarvis ED, Scharff C, Grossman MR, Ramos JA, Nottebohm F. For whom the bird sings: context-dependent gene expression. *Neuron* 21: 775–788, 1998.

Kao MH, Doupe AJ, Brainard MS. Contributions of an avian basal ganglia-forebrain circuit to real-time modulation of song. *Nature* 433: 638–643, 2005.

Kao MH, Wright BD, Doupe AJ. Neurons in a forebrain nucleus required for vocal plasticity rapidly switch between precise firing, and variable bursting depending on social context. *J Neurosci* 28: 13232–13247, 2008.

Kittelberger JM, Mooney R. Lesions of an avian forebrain nucleus that disrupt song development alter synaptic connectivity, and transmission in the vocal premotor pathway. *J Neurosci* 19: 9385–9398, 1999.

Konishi M. The role of auditory feedback in the control of vocalization in the white-crowned sparrow. *Z Tierpsychol* 22: 770–783, 1965.

Lehky SR, Sejnowski TJ, Desimone R. Selectivity, and sparseness in the responses of striate complex cells. *Vision Res* 45: 57–73, 2005.

Leonardo A, Fee MS. Ensemble coding of vocal control in birdsong. *J Neurosci* 25: 652–661, 2005.

Long MA, Fee MS. Using temperature to analyse temporal dynamics in the songbird motor pathway. *Nature* 456: 189–194, 2008.

Long MA, Jin DZ, Fee MS. Support for a synaptic chain model of neuronal sequence generation. *Nature* 468: 394–399, 2010.

Mooney R. Synaptic basis for developmental plasticity in a birdsong nucleus. *J Neurosci* 12: 2464–2477, 1992.

Mooney R, Konishi M. Two distinct inputs to an avian song nucleus activate different glutamate receptor subtypes on individual neurons. *Proc Natl Acad Sci USA* 88: 4075–4079, 1991.

Nottebohm F, Stokes TM, Leonard CM. Central control of song in the canary, *Serinus canarius*. *J Comp Neurol* 165: 457–486, 1976.

Nottebohm F, Kelley DB, Paton JA. Connections of vocal control nuclei in the canary telencephalon. *J Comp Neurol* 207: 344–357, 1982.

Nowak L, Bregestovski P, Ascher P, Herbet A, Prochiantz A. Magnesium gates glutamate-activated channels in mouse central neurones. *Nature* 307: 462–465, 1984.

Ölveczky BP, Andalman AS, Fee MS. Vocal experimentation in the juvenile songbird requires a basal ganglia circuit. *PLoS Biol* 3: e153, 2005.

Perkel DJ. Effects of neuromodulators on excitatory synaptic transmission in nucleus RA of the zebra finch. *Soc Neurosci Abstr* 21: 1995.

Scharff C, Nottebohm F. A comparative study of the behavioral deficits following lesions of various parts of the zebra finch song system: implications for vocal learning. *J Neurosci* 11: 2896–2913, 1991.

Schmidt MF, Perkel DJ. Slow synaptic inhibition in nucleus HVc of the adult zebra finch. *J Neurosci* 18: 895–904, 1998.

Solis MM, Perkel DJ. Noradrenergic modulation of activity in a vocal control nucleus in vitro. *J Neurophysiol* 95: 2265–2276, 2006.

Spiro JE, Dalva MB, Mooney R. Long-range inhibition within the zebra finch song nucleus RA can coordinate the firing of multiple projection neurons. *J Neurophysiol* 81: 3007–3020, 1999.

Stark LL, Perkel DJ. Two-stage, input-specific synaptic maturation in a nucleus essential for vocal production in the zebra finch. *J Neurosci* 19: 9107–9116, 1999.

Stepanek L, Doupe AJ. Activity in a cortical-basal ganglia circuit for song is required for social context-dependent vocal variability. *J Neurophysiol* 104: 2474–2486, 2010.

Sutton RS, Barto AG. Reinforcement Learning: An Introduction. Cambridge, MA: MIT Press, 1998.

Tchernichovski O, Mitra PP, Lints T, Nottebohm F. Dynamics of the vocal imitation process: how a zebra finch learns its song. *Science* 291: 2564–2569, 2001.

Tchernichovski O, Lints T, Mitra PP, Nottebohm F. Vocal imitation in zebra finches is inversely related to model abundance. *Proc Natl Acad Sci USA* 96: 12901–12904, 1999.

Tchernichovski O, Nottebohm F, Ho CE, Pesaran B, Mitra PP. A procedure for an automated measurement of song similarity. *Anim Behav* 59: 1167–1176, 2000.

Thompson JA, Johnson F. HVC microlesions do not destabilize the vocal patterns of adult male zebra finches with prior ablation of LMAN. *Dev Neurobiol* 67: 205–218, 2006.

Tolhurst DJ, Smyth D, Thompson ID. The sparseness of neuronal responses in ferret primary visual cortex. *J Neurosci* 29: 2355–2370, 2009.

Tumer EC, Brainard MS. Performance variability enables adaptive plasticity of 'crystallized' adult birdsong. *Nature* 450: 1240–1244, 2007.

Vicario DS. Organization of the zebra finch song control system. II. Functional organization of outputs from nucleus robustus archistriatalis. *J Comp Neurol* 309: 486–494, 1991.

Vu ET, Mazurek ME, Kuo YC. Identification of a forebrain motor programming network for the learned song of zebra finches. *J Neurosci* 14: 6924–6934, 1994.

Wild JM. Neural pathways for the control of birdsong production. *J Neurobiol* 33: 653–670, 1997.

Yu AC, Margoliash D. Temporal hierarchical control of singing in birds. *Science* 273: 1871–1875, 1996.